International Journal of Fluid Machinery and Systems
Vol. 13, No. 2, April-June 2020
DOI: http://dx.doi.org/10.5293/IJFMS.2020.13.2.327
ISSN (Online): 1882-9554

Original Paper

Numerical Study of Passive and Active Flow Separation Behavior over NACA 0015 Airfoil

Mouhamed Larbi[1], Tayeb Yahiaoui[2], Mustapha Belkadi[1], Lahouari Adjlout[1], Omar Ladjedel[3] and Ondřej Šikula[3]

[1]Laboratoire d"aéro-hydrodynamique navale, Département de génie Maritime, Mechanical Engineering Faculty, USTO Oran, Algeria, mohammed.larbi59@gmail.com, belkadigma@yahoo.fr, adjloutl@yahoo.fr
[2]Laboratoire d"aéronautique et systèmes propulsive, Département de Génie Mécanique, Mechanical Engineering Faculty, USTO Oran, Algeria, yahiaoui_tayeb@yahoo.fr
[3]Brno University of Technology, Faculty of Civil Engineering, Veveří 331/95 Brno 60200, Czechia, lad.omar.univ@gmail.com, sikula.o@vutbr.cz

Abstract

In this paper, numerical investigations are performed to analyze the flow behavior over NACA0015 and the efficiency of vortex generators VGs (triangular and rectangular in shape) and continuous jet as passive and active control devices are evaluated. The unsteady Reynolds-averaged Navier-Stokes equations of the turbulent flow are solved using, k-ω SST provided by the ANSYS CFX-CFD code. The model presented in this paper is a comprehensive representation of the information available in the literature. Validation shows a qualitatively good agreement with previous researches, and almost all flow structures are well reproduced by the computation. The results confirm that the vortex generators can influence flow separation and thus improve the aerodynamic performance of NACA0015 airfoil. The results show that the triangular VGs that include jet are more efficient than the triangular and rectangular VGs.

Keywords: Turbulence, Reynolds number, Drag coefficient, vortex generators.

1. Introduction

Both active and passive controls have been the subject of various researches such as [1-3]. The vortex generators are an important means of passive control, and have been applied in several applications. Control of the boundary layer around the airfoil using vortex generators was presented in the study of Nickerson [4], where the author found that the use of vortex generators (VGs) was advantageous compared to the aerofoil without control due to stall angle increment, and that the vortex generators VGs attached to the surface at 5% chord position have better performance than that at 7.5%. An experimental study by Manolesos and Voutsinas [5] shows that passive vortex generators for wind turbine blades on an airfoil can increase maximum lift by 44%, while drag increases can only reach 0.002 at pre-stall angles of attack. A Comparative analysis of various shapes (rectangle, triangle, and gothic) for a vortex generator for a NACA 0012 Aerofoil was presented by Vasantha et al. [6]. The study shows that triangle-shaped vortex generators give a minimum amount of drag force, and also delay flow separation by increasing velocity near the surface. Tebbiche and Boutoudj [7] proposed new vortex generators (VGs) shape with counter-rotating vortices, in order to increase the lift and decrease drag coefficients by about 14% and 16%, respectively.

The experimental study presented by Betterton et al. [8] shows that a VG size close to a quarter of the boundary layer thickness can significantly reduce the size of regions containing the turbulent boundary layer separated flow. Sok and Lee [9] have studied experimentally flow characteristics and tip vortex formation around a NACA0018 foil with an endplate. Results show that the vortex formation is changed near the end span section due to the prevention of roll-up phenomenon and flow formation around the foil is affected by the end plate until the mid-span. Wong et al [10] conducted an experimental study to determine the effect of plasma vortex generators (PVG) on a NACA 0015 airfoil for flow separation control, and found that this mechanism can increase the lift coefficient by about 6%. Mueller et al [11] conducted an experimental study on the effects of chordwise position, spanwise spacing and VG size with balance force measurements of a 2D wing section. The results obtained show that the best performance of stall suppression was reached with a spacing of Z = 3H. It was found ~~out~~ that an increase of the static stall angle by 12.5◦ with respect to the baseline value was produced with the smaller VG geometry, accompanied by an increase in lift coefficient by 31%.

The numerical and experimental investigations undertaken by Zhen et al. [12] show the effect of triangular and rectangular shaped VGs on the NACA4415 profile regarding aerodynamic performances. In the latter, the spacing between the VGs couple their shape and

Received May 27 2019; revised September 1 2019; accepted for publication January 31 2020:
Review conducted by Zhang Yang-jun. (Paper number O19031C) Corresponding author Ondřej Šikula, sikula.o@vutbr.cz

location, according to the separation point, were investigated. Results show that the maximum lift coefficient of rectangular VGs is higher than that of the triangular one by about 7.8%. Moduki et al [13] investigated a passive control with isolated blading in highly loaded compression cascade at low Mach number. They found that use of this passive control delay the separation and enhance aerodynamic performances of the compression cascade.

Other researchers [14 and 15] have investigated the flow in wing-tip vortex using different turbulence models, they came to the conclusion that the k-ω SST model was the most efficient one for analysing the flow behaviour. Wei Zhang et al. [16] presented results from direct numerical simulations (DNS) of incompressible flow over two airfoils, NACA-4412 and NACA-0012-64, in which the effects of the airfoil geometry on the flow separation and transition patterns at Re=104 and 10 degrees incidence were investigated. Liang and Xue [17] presented the formation of the wing-tip vortex from a rectangular NACA0015 wing with a square tip, in which they compared between an incompressible detached vortex simulation (DES) method and the RANS equations with the SA model respectively. Most of the above researches investigated the different geometries and positions of the VGs. In the present work, a jet is included with different geometries of VGs and compared with the other configurations.

2. Numerical procedure

The flow configuration consists of flow over an NACA0015 airfoil at a Reynolds number of 8.96 105, based on the airfoil chord length and free stream velocity [3]. The flow is considered to be three-dimensional, incompressible, steady, and turbulent. The fluid is taken as air with constant density $\rho = 1.224$ and dynamic viscosity $\mu = 10^{-3}$ Pa.s.

2.1 Geometry and Computational Grid

A passive control of flow around NACA0015 which has a similar configuration to that of the experimental work done by Gilarranz et al. [3] is investigated. The geometry and detailed dimensions and orientations are shown in Figs 1-a, 1-b and presented in table 1.

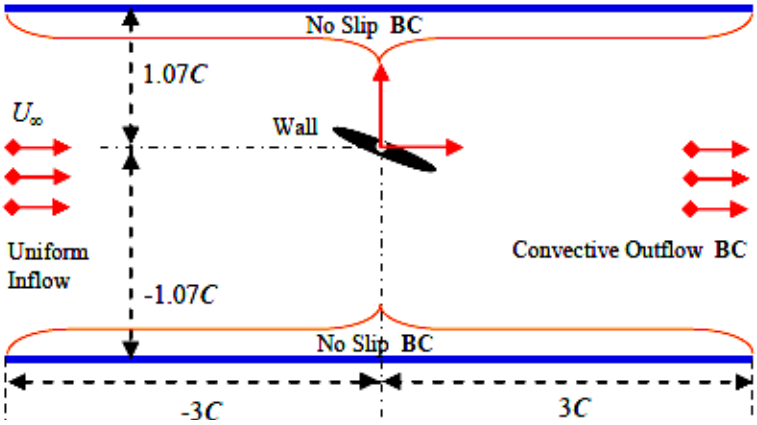

Fig. 1-a Computational domain of flow over an NACA0015 airfoil

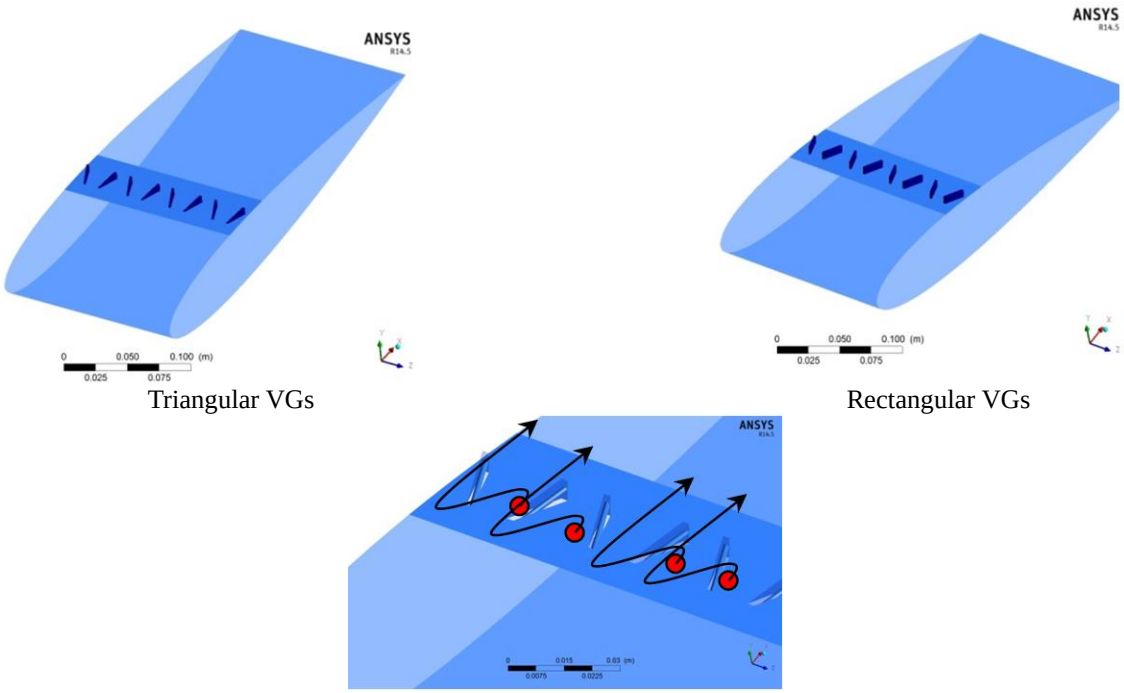

Triangular VGs

Rectangular VGs

Triangular VGs+Jet

Fig. 1-b Details of VGs Triangular, Rectangular and Triangular VGs+Jet [3]

The location and the direction of continuous jet are presented in fig. 2E, where the jet is installed inside the generator vortex at 12% of the leading edge and the angle of the jet is 30°. The jet velocity is fixed taking into account the momentum coefficient

Table 1. Details of VGs

C	375 mm
h	6 mm
l	18 mm
L	40 mm
S	70 mm
β	20°

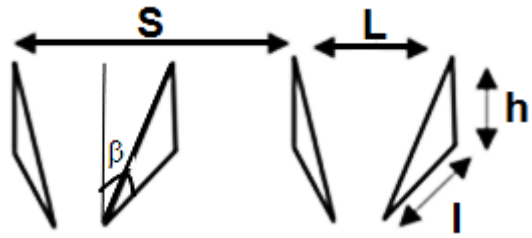

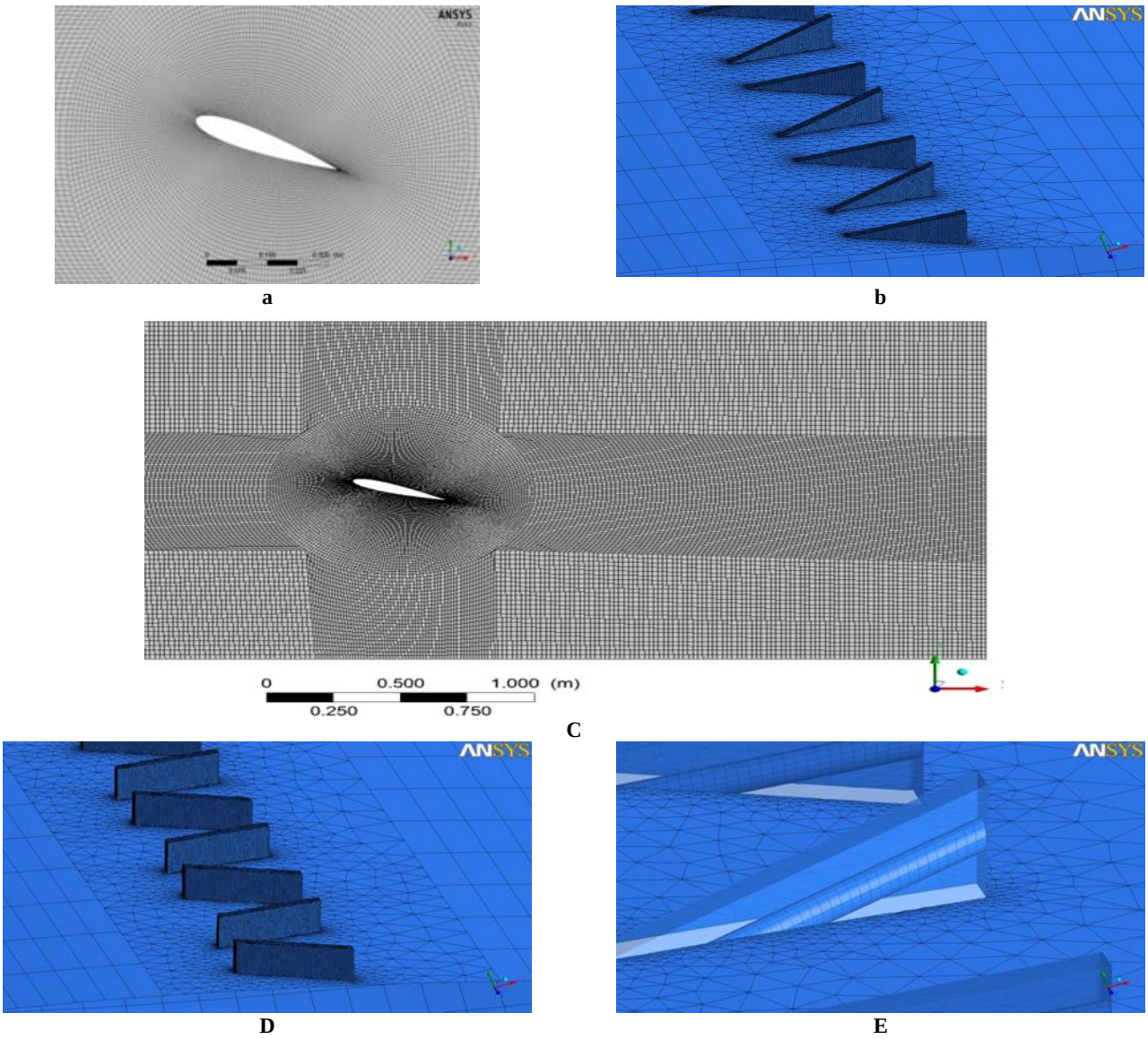

a b C D E

Fig. 2 Vortex generator and mesh configurations in the computational domain

The airfoil NACA0015 with 0.375 m of chord length and external domain were constructed and meshed in ICEM 14.0. A hybrid mesh is adopted, and tetrahedral cells for airfoil and hexahedral cells for external domain are illustrated in Fig. 2.
The flow parameters used in numerical simulation are summarized in table 2. The Reynolds number based on the freestream velocity and the chord length is 8.96 10^5. The freestream Mach number is 0.2. The body fitted mesh has grid points.

The accuracy of the solution of any problem depends on the density and the distribution of the nodes in the mesh. Three grids are generated to test the mesh independence, coarse mesh 1 of 169000 cells, average mesh 2 with 610000 cells and fine mesh 3 of 950000 cells).

Table 2: lift and drag coefficient for each grid.

	Without control	
	Cl	Cd
Experiment (Gilarranz et al [38]	0.82	0.26
Mesh 1	0.75	0.29127
Mesh 2	0.8596	0.25269
Mesh 3	0.8521	0.25914

The mesh 2 will be taken for all subsequent simulations.

Table 3. Computational parameters

Angle of attack	Reynolds number	Grid nodes
16.6°	$8.96*10^5$	610000

2.2 Turbulence modelling

In the present study a numerical investigation of passive control around airfoil NACA0015 has been performed. The Navier-Stokes equations of the turbulent flow are solved using, k-ω SST provided by the ANSYS CFX-CFD code. The flow is considered to be three-dimensional, incompressible, steady, and turbulent. The fluid is Newtonian with constant density ρ and dynamic viscosity μ. The Reynolds Averaged Navier–Stokes (RANS) equations for continuity and momentum conservation can be written as:

$$\frac{\partial(U_i)}{\partial x_i} = 0 \tag{1}$$

$$\frac{\partial(\rho U_j U_i)}{\partial x_j} = \frac{\partial}{\partial x_j}\left(\mu\frac{\partial U_i}{\partial x_j} - \partial\overline{u_i' u_j'}\right) - \frac{\partial p}{\partial x_i} \tag{2}$$

The k-ω SST model by Menter [17] including the low-Reynolds correction is the most used in engineering turbulence modeling for industrial applications. It has a Robust and reasonably accuracy and comprises many sub models for compressibility, buoyancy and combustion.

This model is known to provide a good compromise by combining the k-ω model of Wilcox in the vicinity of the wall region and a high Reynolds k-ε model in the outer region.

$$\frac{\partial(\rho u_j \omega)}{\partial x_j} = \frac{\gamma}{\nu_t} P - \beta\rho\omega^2 + \frac{\partial}{\partial x_j}\left[(\mu + \sigma_\omega \mu_t)\frac{\partial \omega}{\partial x_j}\right] + 2(1 - F_1)\frac{\partial \sigma_{\omega 2}}{\omega}\frac{\partial k}{\partial x_j}\frac{\partial \omega}{\partial x_j} \tag{3}$$

$$\frac{\partial(\rho u_j k)}{\partial x_j} = P - \beta^* \rho\omega k + \frac{\partial}{\partial x_j}\left[(\mu + \sigma_k \mu_t)\frac{\partial k}{\partial x_j}\right] \tag{4}$$

The constant of the k-ω SST model are mentioned below:

$\beta_1 = 0.07,\ \beta_1^* = 0.09,\ \sigma_{k1} = 2,\ \sigma_{\omega 1} = 2,\ \alpha_1 = 5/9$
$\beta_2 = 0.0828,\ \beta_2^* = 0.09\ ,\ \sigma_{k2} = 1,\ \sigma_{\omega 2} = 1/0.856,\ \alpha_2 = 0.44$

3. Results and discussion

The main objective of the numerical investigations presented in this paper is to analyze the flow structure over NACA0015 and to evaluate the efficiency of vortex generators VGs and continuous jet as passive and active control devices. The validation of model testing focus on uncontrolled cases with an angle of attack of 16.6° presented in the previous paper of Gilarranz et al. [3]. As shown in Fig. 3, the simulated results for the pressure coefficient are satisfactorily compared with the experimental data of ref [3].

The comparison of controlled and uncontrolled flow over airfoils at an angle of attack 16.6° is presented in Fig. 4. The VGs effect is clearly shown on the flow behavior comparing with the uncontrolled airfoil. The vortex has been displaced downstream.

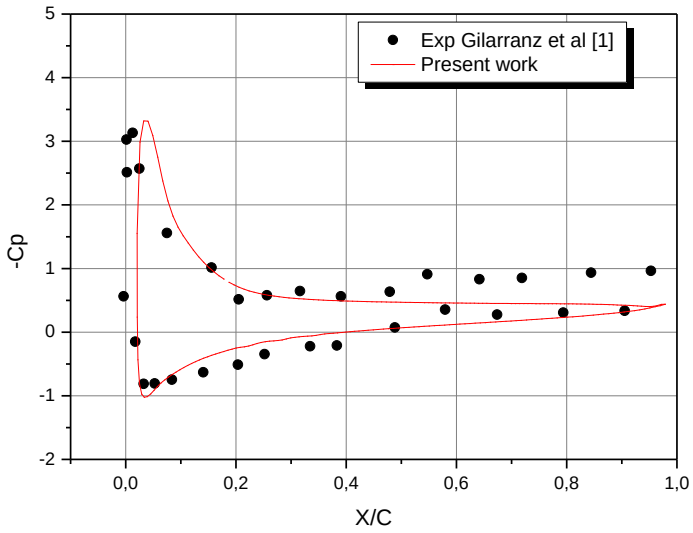

Fig. 3 Comparison between CFD results and experimental data.

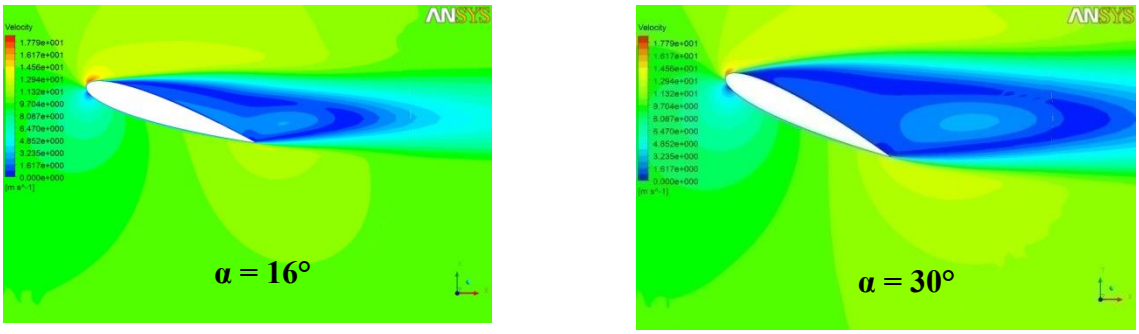

Without control

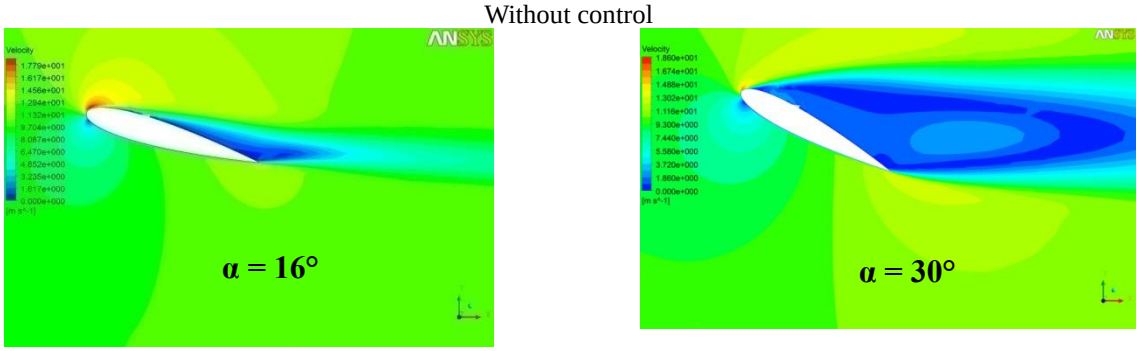

Triangular VGs

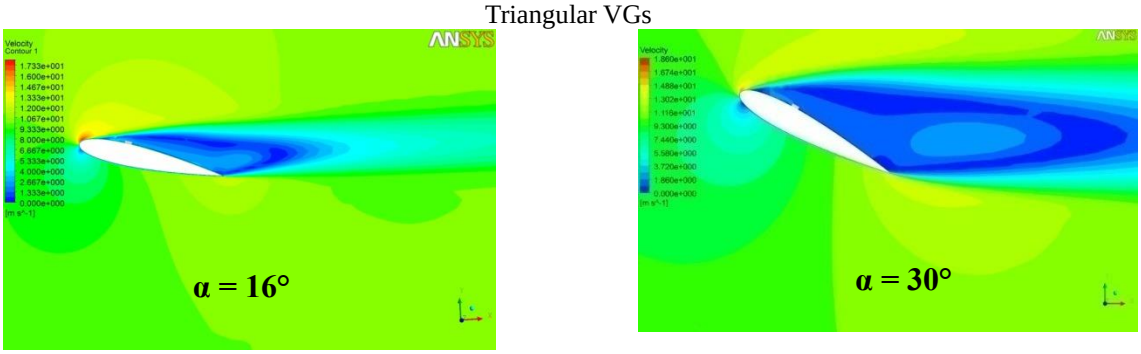

Rectangular VGs

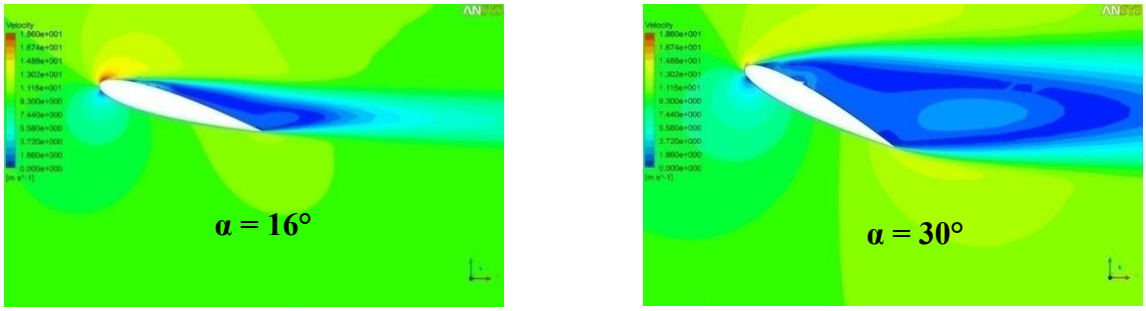

Triangular VGs + Continuous jet

Fig. 4 Velocity contours at different angles

Figure 5 shows the X-velocity contours in the wake region of VGs for α =16.6° and in two positions X/C=0.37 and X/C=0.45. As X increases, counter-rotating vortices gradually expand in the downstream region. Flow in the intermediate region between a converging pair of VGs is in a lower velocity than that between a diverging pair of VGs. The flow in opposite directions generates two counter rotating vortices between a converging pair of VGs.

Pressure coefficient distribution is plotted in fig. 6 at three selected attack angles of, 10°, 24° and 30° and for the controlled flow case. It is clearly seen that the VGs has an effect on the extrados of the airfoil. As can be observed that the use of VGs modifies the pressure coefficient area; this pressure distribution leads to improvement in the aerodynamic performance of the NACA0015.

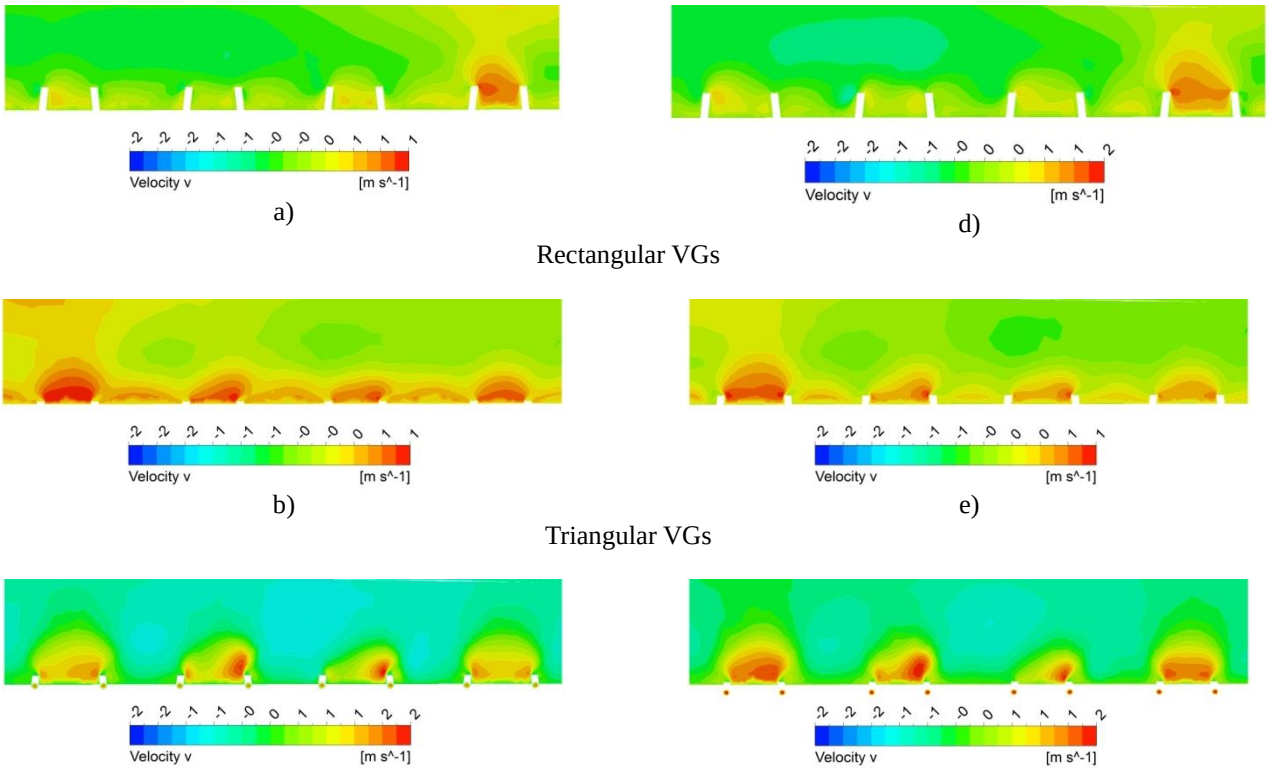

Triangular VGs + Continuous jet

Fig. 5 V-velocity contours in the downstream region of VGs, for α=16.6°
(a-c) X/C=0.37 and (d-f) X/C=0.45

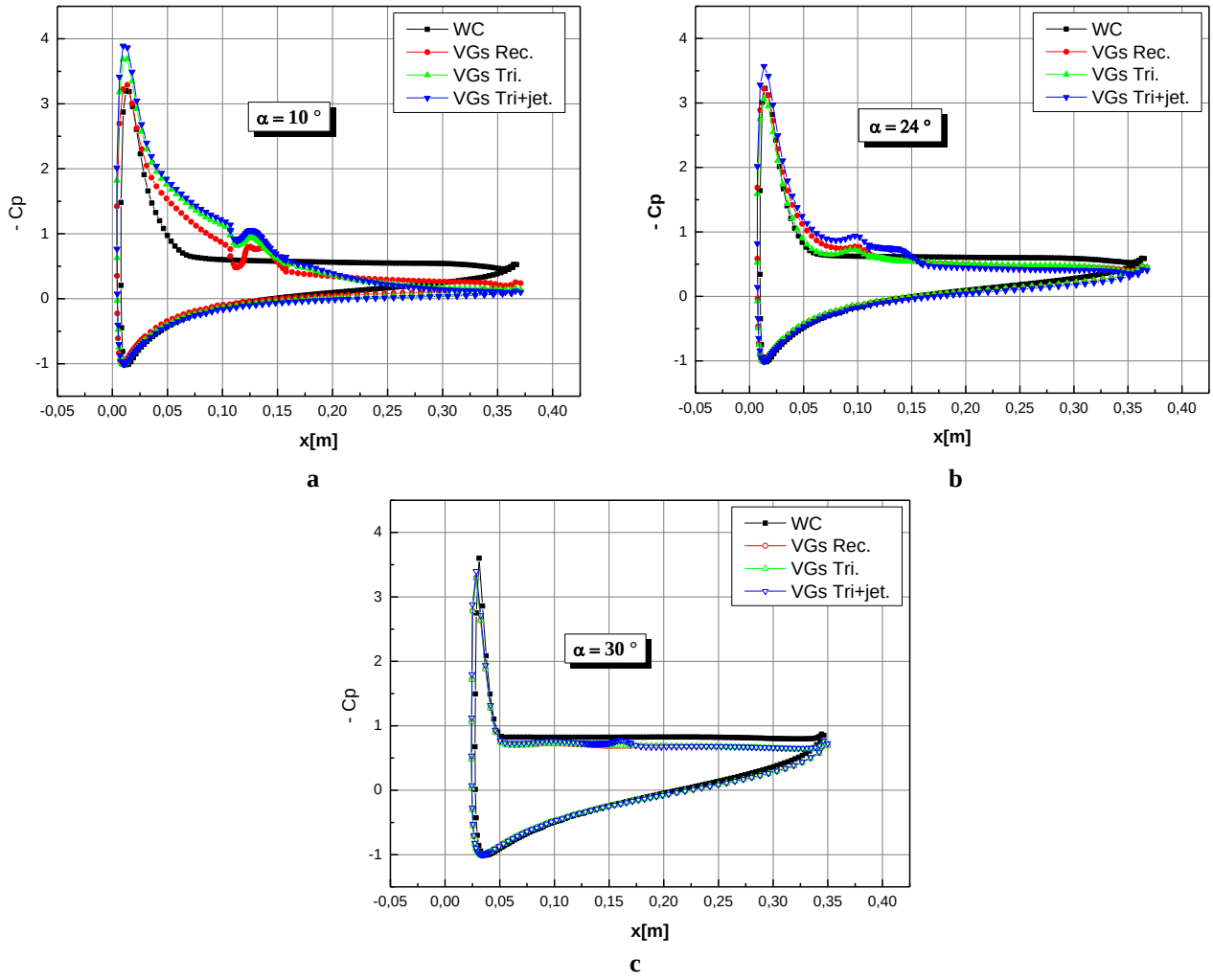

Fig. 6 Comparison of the pressure coefficient

Longitudinal (u) and transversal (v) velocity profiles at the trailing edge of the airfoil are presented on figs. 7, 8 and 9 for angles 16° and 24°. Figures 7 and 8 show typical distributions of u and v through the boundary layer for rectangular VGs, triangular VGs and triangular VGs including jet compared to flow without control (WC). The triangular VGs that include jet significantly enhance the flow around the airfoil.

A range of incidence angle between [-2°, 30°] with increment of 2 degrees are examined to determine the lift and drag coefficients. Each case was simulated with the same Reynolds number (8.96 10^5) to collect the maximum information. Increasing the angle of attack increases lift but it also increases drag, which is a disadvantage. The passive and active control using the triangular VGs including jet (VGs tri+jet) is used in this study to enhance aerodynamic performances of a NACA 0015 airfoil and thus increase the lift coefficient and reduce the drag coefficient as presented in Fig. 10.

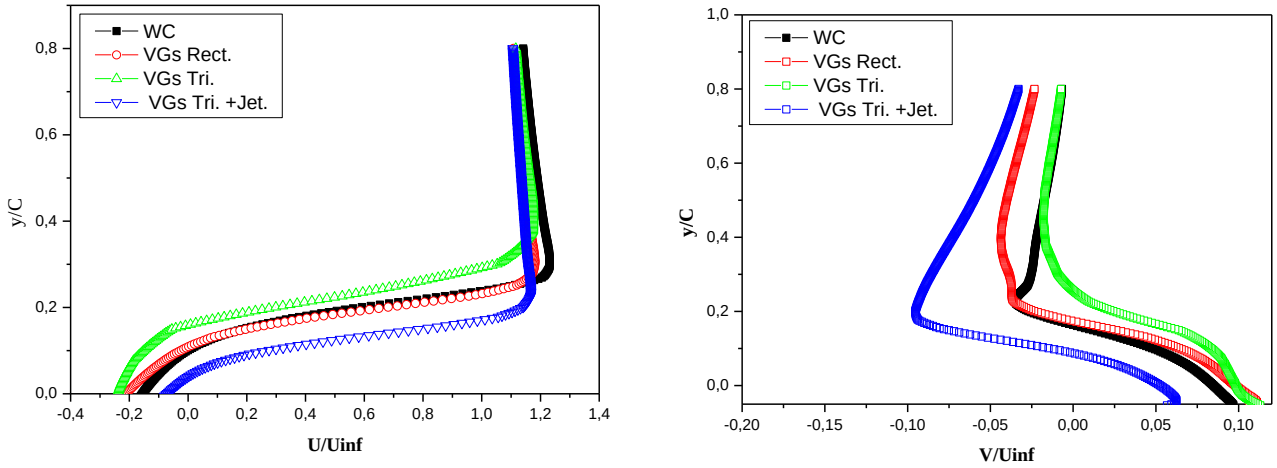

Fig. 7 Longitudinal (u) and transversal (v) velocity profiles for 16°

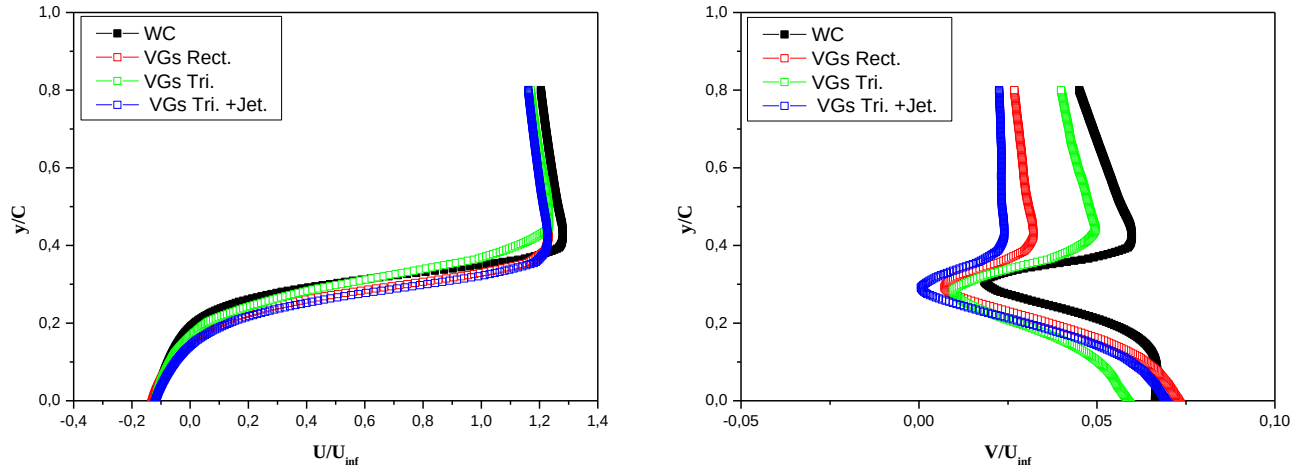

Fig. 8 Longitudinal (u) and transversal (v) velocity profiles for 24°

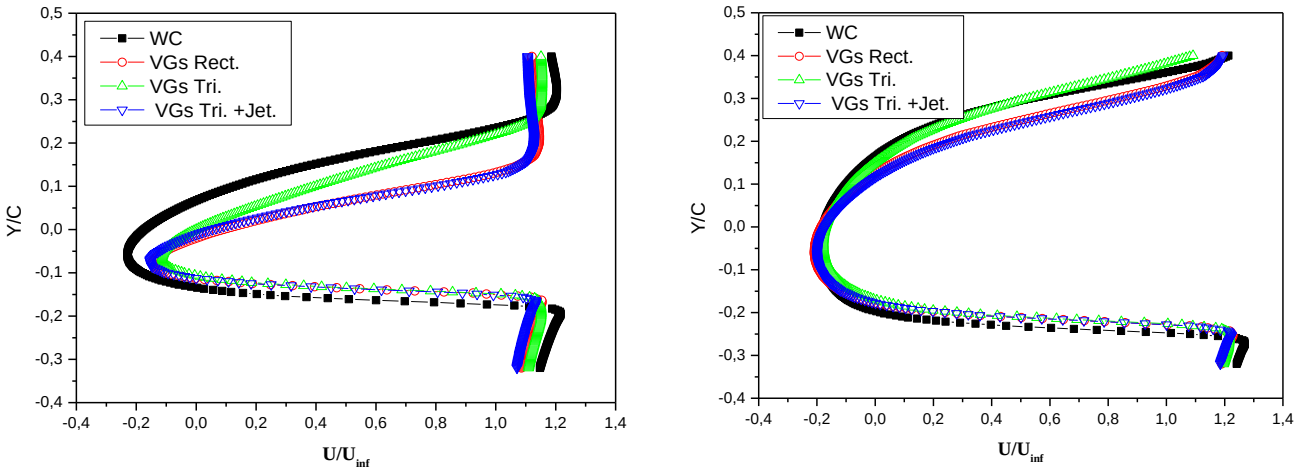

Fig. 9 Longitudinal (u) velocity profiles for 16° and 24°

4. Conclusion

A numerical study has been carried out to investigate the effect of the vortex generators on the aerodynamic performance and the flow behavior around NACA 0015. The u and v velocity, pressure coefficient and lift coefficient were analyzed and discussed. Results show that the use of vortex generators modifies the pressure coefficient area; this pressure distribution leads to improvements in the aerodynamic performance of the NACA0015. For a certain angle of attack, the vortex generators can reduce the recirculation zone of the airfoil and enhance the lift coefficient.

Therefore, vortex generators are able to substantially enhance the aerodynamic performance of airfoil NACA 0015 and be subsequently used as performance devices.

Acknowledgments

The research was supported by grants GA 19-20943S and GA 20-00630S funded by the Czech Science Foundation.

References

[1] Linyue Gao, Hui Zhang, Yongqian Liu, Shuang Han., 2015, “Effects of vortex generators on a blunt trailing-edge airfoil for wind turbines,” Renewable Energy, 76 , 303-311.

[2] Lei Zhang, Xingxing Li, Ke Yang, Dingyun Xue., 2016, “Effects of vortex generators on aerodynamic performance of thick wind turbine airfoils,” J Wind Eng Ind Aerodyn, 156, 84–92.

[3] Gilarranz, Traub, Rediniotis., 2005, “A new class of synthetic jet actuators-partII: application to flow separation control,” ASME Journal of Fluids Engineering 127, 377–387.

[4] Nickerson J. D. Jr. , 1986, “A study of vortex generators at low Reynolds numbers,” AIAA 24th Aerospace Sciences Meeting, January 6-9, Reno, Nevada.

[5] Marinos Manolesos n, SpyrosG.Voutsinas., 2015, “Experimental investigation of the flow past passive vortex generators on an airfoil experiencing three-dimensional separation,” J. Wind Eng. Ind. Aero dyn.142, 130–148.

[6] G.Vasantha, K.Sathiya, S.Aravindhkumar, S.KishoreKumar., 2016, “Comparative Analysis of Various Vortex Generators for a

NACA 0012 Aerofoil," I J of Innovative Studies in Sciences and Engineering Technology, 2.
[7] H. Tebbiche, M. Boutoudj., 2014, "Optimized vortex generators in the flow separation control around a NACA 0015 profile," EURODYN.
[8] J. Betterton, K.Hackett, P.Ashill, MJ.Wilson, I. Woodcock, C.Tilman, and K.Langan. , 2000, "Laser doppler anemometry investigation on sub boundary layer vortex generators for flow control," In 10th symposium on application of laser techniques to fluid mechanics, Lisbon, 10–12.
[9] Ok-Sok Gim and Gyoung-WooLee., 2016, "Flow characteristics and tip vortex formation around a NACA0018foil with an end plate," J Ocean Engineering, 60, 28–38.
[10] C. W. Wong, Y. Zhou, Y. Z. Li and B. F. Zhang., 2015, "Skin Friction Drag Reduction Based on Plasma-Induced Streamwise Vortices," Fluid-Structure-Sound Interactions and Control, 139-144.
[11] H. Mueller, G. Pechlivanoglouvortex, C.N. Nayeri and C.O. Paschereit., 2012, "generators for wind turbine blades: a combined wind tunnel and wind turbine parametric study," Proceedings of ASME Turbo Expo.
[12] T. Zhen, M. Zubair, K. Ahmad., 2011, "Experimental and numerical investigation of the effects of passive vortex generators on aludra UAV performance," Chin. J. Aeronaut. 24, 577–583.
[13] Mdouki Ramzi, Gérard Bois and Gahmousse Abderrahmane ,2011, "Numerical Study of Passive Control with Slotted Blading in Highly Loaded Compressor Cascade at Low Mach number," International Journal of Fluid Machinery and Systems 4(1), 97-103.
[13] J. Churchfield and A. Blaisdell., 2013, "A Reynolds Stress Relaxation Turbulence Model Applied to A Wingtip Vortex Flow," AIAA Journal, 51, 2643-2655.
[14] P. R. SpalartM, L. Shur, M. Kh and A. K. Travin., 2015, "Direct Simulation and RANS Modelling of a Vortex Generator Flow," 95, 335–350.
[15] Wei Zhang, Wan Cheng, Wei Gao, Adnan Qamar, Ravi Samtaney., 2015, "Geometrical effects on the airfoil flow separation and transition," J Computers & Fluids, 116, 60–73.
[16] Z. Liang and L. Xue., 2014, "Detached-eddy simulation of wing-tip vortex in the near field of NACA 0015 airfoil," J of Hydrodynamics, 26, 199-206.